

EXAFS Study of Two-Dimensional Organic/Inorganic Hybrid Nanocomposites, $\text{Cu}_2(\text{OH})_3(n\text{-C}_m\text{H}_{2m+1}\text{COO})$ ($m = 0, 1, 7, 8, 9$): Structural Modification in the Inorganic Layer Induced by the Interlayer Organic Molecule

Wataru Fujita,[†] Kunio Awaga,^{*,†} and Toshihiko Yokoyama[‡]

Department of Basic Sciences, Graduate School of Arts and Sciences, The University of Tokyo, Komaba, Meguro-ku, Tokyo 153, Japan, and Department of Chemistry, School of Science, The University of Tokyo, Hongo, Bunkyo-ku, Tokyo 113, Japan

Received July 3, 1996[⊗]

The local structures of the two-dimensional organic/inorganic hybrid nanocomposites, $\text{Cu}_2(\text{OH})_3(n\text{-C}_m\text{H}_{2m+1}\text{COO})$ ($m = 0, 1, 7, 8, 9$), have been investigated, together with $\text{Cu}_2(\text{OH})_3\text{NO}_3$, by means of Cu K-edge EXAFS spectroscopy at 20 K. The axial and equatorial Cu–O bond lengths, three kinds of Cu–Cu distances, and their Debye–Waller factors have been determined. The structural parameters for $\text{Cu}_2(\text{OH})_3\text{NO}_3$ agree with those determined by the previous X-ray crystal analyses. The $\text{Cu}_2(\text{OH})_3(n\text{-C}_m\text{H}_{2m+1}\text{COO})$ materials are found to maintain the basic framework of the inorganic layer, but from a microscopic viewpoint, there is a characteristic difference in the local structures between the shorter ($m = 0, 1$) and the longer ($m = 7–9$) alkyl chain materials. While the local structures of the $m = 0$ and 1 materials are very similar to that of $\text{Cu}_2(\text{OH})_3\text{NO}_3$, those of $m = 7–9$ exhibit a significant shortening of the axial Cu–O bond length by $\sim 0.1 \text{ \AA}$, in contrast to little change in the equatorial length. Since the interlayer alkanecarboxylate is always in the axial position, the change is ascribed to the shorter Cu–carboxylate bond length in the longer chain materials. The structural modifications in the other parts of the layer can be understood as a cooperative motion originating from the change. It is quite unusual that such a large structural modification of an inorganic layer takes place, depending on the intercalated organic molecules. The intralayer structural modification observed in this study is sufficiently large enough to explain the reported drastic change in the magnetic properties between the shorter and longer chain materials.

Introduction

Intercalation of organic molecules into inorganic layered materials is a recent matter of concern.¹ The interlayer space may allow the organic molecule to show new chemical and/or physical properties far from those in the bulk crystal. Modification of the physical properties of the inorganic layer caused by the intercalation and cooperative phenomena between the organic and the inorganic substances are also interesting.

Basic copper hydroxides, $\text{Cu}_2(\text{OH})_3\text{X}$ ($\text{X} = \text{NO}_3$, carboxylate, and so on), attract much interest as heterogeneous catalysts² and as two-dimensional magnetic materials³ because of their lamellar structure. As schematically shown in Figure 1, the material exhibits a botallackite-type structure, in which two crystallographically distinct copper atoms (Cu^{i} and Cu^{ii}) lie in $4\text{O}^{\text{i}} + 2\text{O}^{\text{iii}}$ and $4\text{O}^{\text{i}} + 1\text{O}^{\text{ii}} + 1\text{O}^{\text{iii}}$ environments, respectively,

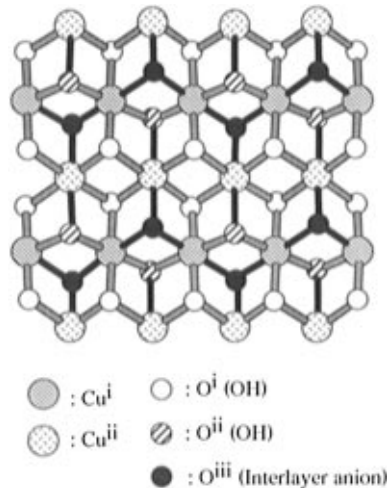


Figure 1. Schematic view of the copper hydroxide layer in $\text{Cu}_2(\text{OH})_3\text{X}$.

with a Jahn–Teller distortion.⁴ The dark gray sticks in Figure 1 show the prolonged axial Cu–O bonds, and the light gray ones are the bonds in the equatorial planes. The counteranion X is located in the interlayer and coordinates the copper ion. It is known that the anion is exchangeable with various organic anions, and various intercalation compounds can easily be produced.⁵

In the previous article,⁶ we described that the magnetic properties of the copper hydroxyalkancarboxylate series, $\text{Cu}_2(\text{OH})_3(n\text{-C}_m\text{H}_{2m+1}\text{COO})$ ($m = 0, 1, 7, 8, 9$), drastically depend

[†] Department of Basic Sciences.

[‡] Department of Chemistry.

[⊗] Abstract published in *Advance ACS Abstracts*, December 15, 1996.

- (1) (a) Ozin, G. A. *Adv. Mater.* **1992**, *4*, 612. (b) O'Hare D. *New J. Chem.* **1994**, *18*, 989. (c) Nicoud, J.-F. *Science* **1994**, *263*, 638.
- (2) Mitchell, I. V. *Pillared Layered Structures: Current Trends and Applications*; Elsevier Applied Science Ltd.: London, 1990.
- (3) (a) Takada, T.; Bando, Y.; Kiyama, M.; Miyamoto, H. *J. Phys. Soc. Jpn.* **1966**, *21*, 2726. (b) Takada, T.; Bando, Y.; Kiyama, M.; Miyamoto, H. *J. Phys. Soc. Jpn.* **1966**, *21*, 2745. (c) Miyamoto, H.; Shinjo, T.; Bando, Y.; Takada, T. *J. Phys. Soc. Jpn.* **1967**, *23*, 1421. (d) Enoki, T.; Tsujikawa, I. *J. Phys. Soc. Jpn.* **1975**, *39*, 317. (e) Rabu, P.; Angelov, S.; Legoll, P.; Belaiche, M.; Drillon, M. *Inorg. Chem.* **1993**, *32*, 2463. (f) Drillon, M.; Hornick, C.; Laget, V.; Rabu, P.; Romero, F. M.; Rouba, S.; Ulrich, G.; Ziessel, R. *Mol. Cryst. Liq. Cryst.* **1995**, *273*, 125.
- (4) (a) Wells, A. F. *Acta Crystallogr.* **1949**, *2*, 175. (b) Oswald, H. R.; Feiknecht, W. *Helv. Chim. Acta* **1964**, *47*, 272 and references therein. (c) Jiménez-López, A.; Rodríguez-Castellón, E.; Olivera-Pastor, P.; Maireles-Torres, P.; Tomlinson, A. A. G.; Jones, D. J.; Rozière, J. J. *Mater. Chem.* **1993**, *3*, 303.

- (5) (a) Yamanaka, S.; Sako T.; Hattori, M. *Chem. Lett.* **1989**, 1869. (b) Yamanaka, S.; Sako T.; Seki, K.; Hattori, M. *Solid State Ionics* **1992**, *53–56*, 527.

- (6) Fujita, W.; Awaga, K. *Inorg. Chem.* **1996**, *35*, 1915.

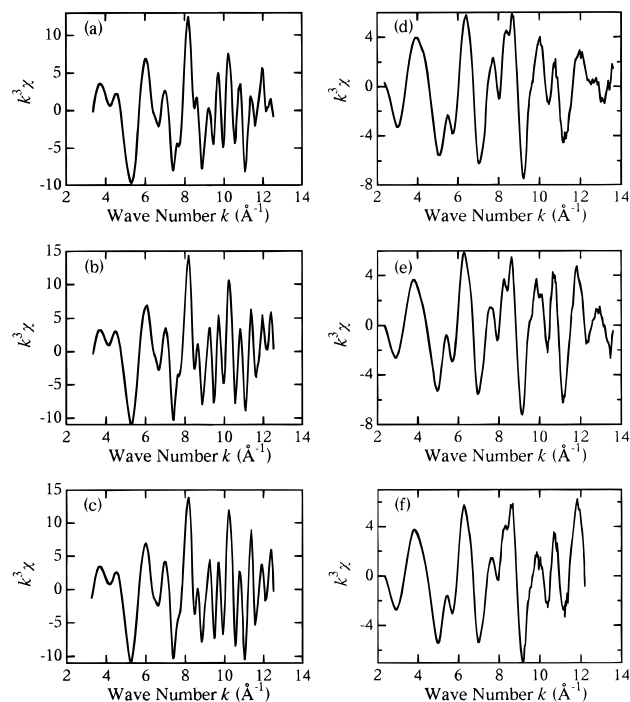


Figure 2. Cu K-edge EXAFS oscillation functions $k^3\chi(k)$ of $\text{Cu}_2(\text{OH})_3\text{NO}_3$ (a) and the $\text{Cu}_2(\text{OH})_3(n\text{-C}_m\text{H}_{2m+1}\text{COO})$ series measured at 20 K: $m = 0$ (b); $m = 1$ (c); $m = 7$ (d); $m = 8$ (e); $m = 9$ (f).

on the alkyl chain length: the shorter chain materials ($m = 0, 1$) exhibit a metamagnetic behavior, which consists of a stronger ferromagnetic interaction and a weaker antiferromagnetic interaction, while the longer chain materials ($m = 7-9$) are weak ferromagnets of $T_N = 22$ K with an intense antiferromagnetic interaction. The primary magnetic interaction changes from ferromagnetic to antiferromagnetic with the extension of the chain.

X-ray absorption spectroscopy is a useful tool for determining the structure of a powder sample. Extended X-ray absorption fine structure (EXAFS) is sensitive to the local environment around the specific atoms that absorb X-rays. EXAFS analysis gives information on the type and number of nearest-neighboring atoms around the X-ray-absorbing atoms and the average interatomic distances with an accuracy of ± 0.02 Å. In the present study, we investigated the local structures of the $\text{Cu}_2(\text{OH})_3(n\text{-C}_m\text{H}_{2m+1}\text{COO})$ ($m = 0, 1, 7, 8, 9$) series, together with $\text{Cu}_2(\text{OH})_3\text{NO}_3$ as a standard, using Cu K-edge EXAFS. The structural difference in the series is discussed, based on the obtained effective coordination numbers, interatomic distances, and Debye–Waller factors.

Experimental Section

The intercalation compounds $\text{Cu}_2(\text{OH})_3(n\text{-C}_m\text{H}_{2m+1}\text{COO})$ ($m = 0, 1, 7, 8, 9$) were prepared according to ref 6. The standard sample $\text{Cu}_2(\text{OH})_3\text{NO}_3$ was obtained by means of the ion-exchange method given in ref 5.

EXAFS measurements were performed using the hard X-ray XAFS station BL-10B of the Photon Factory in National Laboratory for High Energy Physics (2.5 GeV, 350–250 mA).⁷ The samples were diluted with boron nitride to make pellets with a diameter of 20 mm. Cu K-edge spectra were taken using a Si (311) channel-cut monochromator with the transmission mode at 20 K. The intensities of the incident and transmitted X-rays were measured with ionization chambers filled with N_2 and Ar, respectively.

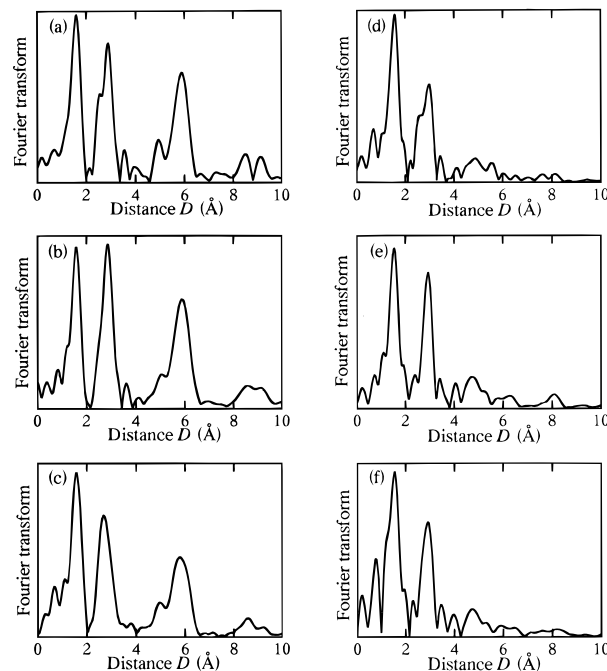


Figure 3. Fourier transforms of $k^3\chi(k)$ of $\text{Cu}_2(\text{OH})_3\text{NO}_3$ (a) and the $\text{Cu}_2(\text{OH})_3(n\text{-C}_m\text{H}_{2m+1}\text{COO})$ series: $m = 0$ (b); $m = 1$ (c); $m = 7$ (d); $m = 8$ (e); $m = 9$ (f).

Data analyses for experimental spectra were performed by standard procedures⁸ using the program EXAFSH by Yokoyama et al.⁹ The EXAFS oscillation function $\chi(k)$ was at first extracted by the background subtraction in the pre- and postedge regions and subsequent normalization using the atomic absorption coefficient. The edge energy E_0 was tentatively given as 8993.51 eV, which was the inflection point of the standard $\text{Cu}_2(\text{OH})_3\text{NO}_3$ spectrum. The resulting EXAFS spectra were k^3 -weighted in order to compensate for the attenuation of the EXAFS amplitude at high k regions and then Fourier-transformed into r space in the range of $\Delta k = 3.35-12.51$ Å⁻¹ for the NO_3 , $m = 0$ and 1 materials, 2.35–13.60 Å⁻¹ for the $m = 7$ and 8 materials, and 2.35–12.20 Å⁻¹ for the $m = 9$ material. The $k^3\chi(k)$ functions and their Fourier transforms are depicted in Figures 2 and 3.

The structural parameters were determined for the shells of interest. The Fourier peaks were filtered multiplying by a Hanning window function and were then inverse Fourier-transformed in k space again in the range of $\Delta R = 1.20-3.30$ Å. A resultant $\chi(k)$ was curve-fitted by using the following standard formula,

$$\chi_{\text{theor}}(k) = s_0 \sum A_i(k) \sin[2kD_i + \phi_i(k)] \quad (1)$$

where D_i and $\phi_i(k)$ are the averaged interatomic distance and the total phase shift of the i th shell and s_0 is the intrinsic loss factor. The amplitude $A_i(k)$ in eq 1 can be expressed as

$$A_i(k) = (N_i/kD_i^2)F_i(k) \exp(-2k^2\sigma_i^2) \quad (2)$$

where N_i is the effective coordination number, σ_i^2 is the EXAFS Debye–Waller factor, and $F_i(k)$ is the backscattering amplitude. The $F_i(k)$ and $\phi_i(k)$ have been theoretically calculated by a curved wave ab initio EXAFS code FEFF6,¹⁰ assuming the model of binuclear copper compound bridged by two oxygen atoms.

In the course of EXAFS fitting between the experimental and the theoretical spectra, N_i and ΔE_{0i} were fixed as shown in Tables 1 and 2, and s_0 was assumed to be 1. The distances of Cu–O(1), Cu–O(2),

- (8) Koningsberger, D. C.; Prins, R. *X-Ray Absorption: Principles, Applications, Techniques of EXAFS, SEXAFS and XANES*; John Wiley & Sons: New York 1988.
- (9) Yokoyama, T.; Hamamatsu, H.; Ohta, T. Program EXAFSH Version 2.1, The University of Tokyo, 1994.
- (10) (a) Rehr, J. J.; de Leon, J. M.; Zabinsky, S. I.; Albers, R. C. *J. Am. Chem. Soc.* **1991**, *113*, 5135. (b) Zabinsky, S. I.; Rehr, J. J.; Ankudinov, A.; Albers, R. C.; Eller, M. J. *Phys. Rev.* **1995**, *B46*, 2995.

(7) (a) Oyanagi, H.; Matsushita, T.; Ito, M.; Kuroda, H. *KEK-Rep.* **1984**, 83/30. (b) Nomura, M.; Koyama, A. *KEK-Rep.* **1989**, 89/16.

Table 1. Comparison between the EXAFS and Single-Crystal Analyses on $\text{Cu}_2(\text{OH})_3\text{NO}_3$

	EXAFS data				diffraction data ^a $D_{\text{diff}}/\text{\AA}$
	N	$\Delta E_0/\text{eV}$	$D_{\text{EXAFS}}/\text{\AA}^b$	$\sigma^2/\text{\AA}^2$ ^b	
Cu—O(1)	4	1	1.98	0.0094	1.929–2.018
Cu—N(2)	2	10	2.38	0.0230	2.309–2.480
Cu—Cu(1)	2	–8	3.02	0.0029	3.044, 3.045
Cu—Cu(2)	2	–8	3.15	0.0026	3.144, 3.146
Cu—Cu(3)	2	–8	3.25	0.0078	3.217, 3.236
$R = 0.044^c$					

^a Reference 9b. ^b Fitting accuracy is ~ 0.02 Å for the distance and 25% for the Debye–Waller factor. ^c The residual factor R is defined as $[\sum(k^3\chi_{\text{exp}}(k) - k^3\chi_{\text{theor}}(k))^2/\sum(k^3\chi_{\text{exp}}(k))^2]^{1/2}$.

Cu—Cu(1), Cu—Cu(2), and Cu—Cu(3) pairs (see Figure 4) and the corresponding Debye–Waller factors were optimized.

Results and Discussion

Standard Sample. The EXAFS oscillation function and the corresponding Fourier transform of the standard sample $\text{Cu}_2(\text{OH})_3\text{NO}_3$ are shown in Figures 2a and 3a, respectively. One can see the distribution of the interatomic distances in the direct space in the latter figure. The two principal peaks at ~ 2 and 3 Å in the Fourier transforms are assigned to the Cu—O and Cu—Cu contributions, respectively. The intense peak at ~ 6 Å is assignable to the next Cu—Cu shell in the copper–hydroxide layers which is intensified by the linear Cu—Cu—Cu arrangement.¹¹ Table 1 shows the effective coordination numbers, the interatomic distances, and the EXAFS Debye–Waller factors obtained in the analyses. The distances Cu—O(1) and Cu—O(2) are equatorial and axial bond lengths, respectively. The distance Cu—Cu(1) is between two identical Cu ions, namely, between $\text{Cu}^{\text{i}}-\text{Cu}^{\text{i}}$ or between $\text{Cu}^{\text{ii}}-\text{Cu}^{\text{ii}}$, and Cu—Cu(2) and Cu—Cu(3) are the two different $\text{Cu}^{\text{i}}-\text{Cu}^{\text{ii}}$ distances. The table also includes the results of the X-ray structure analyses on the single crystal.¹² There are eight and four crystallographically independent distances, respectively, for the equatorial and axial Cu—O bond lengths in the single crystal. However, the difference among the equatorial lengths or between the axial lengths seems to be out of the precision of usual EXAFS analyses, and we adopted two different distances as the fitting parameters for the equatorial and axial bond lengths, ignoring the site-dependent difference. As shown in Table 1, the obtained Cu—O distances are 1.98 Å with $\sigma^2 = 0.0094$ Å² for the equatorial bond length and 2.38 Å with $\sigma^2 = 0.0230$ Å² for the axial one, both of which agree with the corresponding single-crystal data within experimental errors. Concerning the three Cu—Cu distances, quite reasonable agreements are also obtained. The EXAFS analyses in this work were thus justified by the comparison with the single-crystal data on the standard sample.

$\text{Cu}_2(\text{OH})_3(n-\text{C}_m\text{H}_{2m+1}\text{COO})$ Series. Panels b–f of Figure 3 show the EXAFS oscillation functions of the $\text{Cu}_2(\text{OH})_3(n-\text{C}_m\text{H}_{2m+1}\text{COO})$ ($m = 0, 1, 7, 8, 9$) series, respectively. Panels b–f of Figure 4 give the corresponding Fourier transforms. The spectra clearly indicate that the local environments of the copper atom in the shorter alkyl chain materials ($m = 0, 1$) are similar to that in the standard but are quite different from those in the longer chain materials ($m = 7–9$). The most characteristic difference of the longer chain materials is the absence of the ~ 6 Å peak in the Fourier transforms. Since moiré image interference was observed in the TEM photographs of the longer

chain materials,¹³ the absence is not caused by disorder effects in the $[\text{Cu}_2(\text{OH})_3]^+$ layer upon intercalation of the longer alkanecarboxylates. It would be due to a zigzag array of the Cu atoms.

The EXAFS data were treated by the same method as the standard. We also tried to analyze the data with fewer parameters, two Cu—O and single Cu—Cu distances and their Debye–Waller factors, but we could not optimize the fitting parameters for all the samples. The obtained structural parameters are summarized in Table 2. The values of the $\text{Cu}_2(\text{OH})_3(n-\text{C}_m\text{H}_{2m+1}\text{COO})$ series entirely resemble those of $\text{Cu}_2(\text{OH})_3\text{NO}_3$, indicating that the framework of the two-dimensional structure shown in Figure 1 is maintained in the series. Particularly, the coordination environments of the shorter chain compounds are very similar to that of $\text{Cu}_2(\text{OH})_3\text{NO}_3$. However, the longer chain materials show a characteristic modification. The most significant change around the Cu ion is the shortening of the axial Cu—O bond length, namely, Cu—O(2), by ~ 0.1 Å, in contrast to little change of the equatorial bond length, Cu—O(1). Because the carboxylate occupies half of the axial positions in the layer (see Figure 1), the closer Cu—O(2) distance implies the shorter Cu—carboxylate bond length in the $m = 7–9$ materials. In the previous study,⁶ the shorter and longer chain materials are indicated to provide monolayer and bilayer structures in the organic layer, respectively. The difference in the intermolecular arrangement of the alkyl groups in the interlayer could result in the orientational difference of the carboxylate group with respect to the octahedra and in the difference in the Cu—O(2) distance. Concerning the Cu—Cu distances, Cu—Cu(1), and Cu—Cu(3) show clear shortening, while Cu—Cu(2) becomes slightly longer. This change can be explained by a reasonable increase in the angle between Cu—Cu(1) and Cu—Cu(3), denoted as α in Figure 4, by $\sim 8^\circ$. Two neighboring Cu^{i} ions are connected by the oxygen of the alkanecarboxylate. The Cu—Cu(1) distance, the average of the $\text{Cu}^{\text{i}}-\text{Cu}^{\text{i}}$ and $\text{Cu}^{\text{ii}}-\text{Cu}^{\text{ii}}$ ones, should be shortened, associated with the contraction of the axial Cu—O(2) bond length, although the distance between $\text{Cu}^{\text{ii}}-\text{Cu}^{\text{ii}}$ is not bridged by the oxygen. The contraction of the Cu—Cu(3) distance can also be understood because of the alkanecarboxylate bridge, similar to that of Cu—Cu(1). On the other hand, Cu—Cu(2) does not include the carboxylate bridge but only hydroxo one as shown in Figure 4.

These changes indicate that the axial bonds rotate toward the 2-D plane and the dihedral angle between the 2-D plane and the equatorial plane becomes larger, because of the shortening of the axial Cu—O(2) bond, which includes the carboxylate bridge. This fact is consistent with the contractions of the Cu—Cu(1) and Cu—Cu(3) interatomic distances which are bridged by the alkanecarboxylate. The structural modification between the shorter and longer chain materials can be understood simply by the contraction of the two axial bonds, which is caused by a stronger “chemical pressure” from the longer alkyl chain.

It is quite unusual that such a large structural modification of inorganic layers is observed upon intercalation of organic molecules. For instance, the structural modifications upon intercalation of organic molecules have been studied by means of EXAFS on $\text{Rb}_{0.28}\text{NbSe}_2$,¹⁴ $\text{MnPS}_3\text{CoCp}^{2+}$,¹⁵ FeOCID ($D = \text{TTF}$, TTN , TTT , TMTSF),¹⁶ and $\text{FeOCl}_{1-x}(\text{OR})_x$ ($R = \text{CH}_3$ or

(13) Unpublished data.

(14) Bourdillon, A. J.; Pettifer, R. F.; Marseglia, E. A. *Physica* **1980**, *99B*, 64.

(15) Michalowicz, A.; Clément, R. *Inorg. Chem.* **1982**, *21*, 3872.

(16) Kauzlarich, S. M.; Teo, B. K.; Averill, B. A. *Inorg. Chem.* **1986**, *25*, 1209.

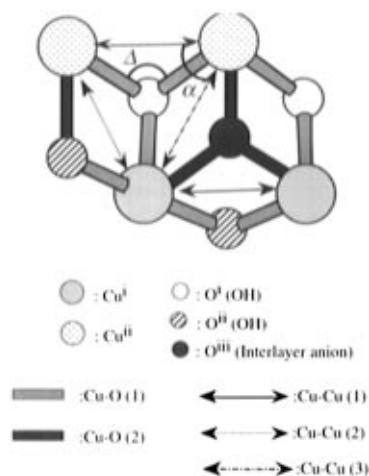
(11) Teo, B. K. *EXAFS, Principles and Data Analysis*; Springer-Verlag Ltd.: Berlin, 1986.

(12) Effenberger, H. *Z. Kristallogr.* **1983**, *165*, 127. (b) Bovio, B.; Locchi, S. J. *Cryst. Spectrosc. Res.* **1982**, *12*, 507.

Table 2. Local Structure Parameters of $\text{Cu}_2(\text{OH})_3(n\text{-C}_m\text{H}_{2m+1}\text{COO})$ ($m = 0, 1, 7, 8, 9$)

	N	$\Delta E_0/\text{eV}$	$m = 0$		$m = 1$		$m = 7$		$m = 8$		$m = 9$	
			$D/\text{\AA}^a$	$\sigma^2/\text{\AA}^2$ ^a	$D/\text{\AA}$	$\sigma^2/\text{\AA}^2$	$D/\text{\AA}$	$\sigma^2/\text{\AA}^2$	$D/\text{\AA}$	$\sigma^2/\text{\AA}^2$	$D/\text{\AA}$	$\sigma^2/\text{\AA}^2$
Cu–O(1)	4	1	1.98	0.0093	1.99	0.0097	1.97	0.0101	1.98	0.0115	1.98	0.0112
Cu–O(2)	2	10	2.43	0.0286	2.38	0.0282	2.28	0.0170	2.29	0.0131	2.29	0.0156
Cu–Cu(1)	2	–8	3.03	0.0018	3.03	0.0025	2.84	0.0117	2.84	0.0082	2.85	0.0098
Cu–Cu(2)	2	–8	3.16	0.0003	3.16	0.0005	3.28	0.0117	3.29	0.0143	3.28	0.0142
Cu–Cu(3)	2	–8	3.27	0.0060	3.26	0.0054	3.00	0.0079	3.01	0.0048	3.01	0.0059
			$R = 0.056^b$		$R = 0.036$		$R = 0.079$		$R = 0.082$		$R = 0.072$	

^a Fitting accuracy is ~ 0.02 Å for the distance and 25% for the Debye–Waller factor. ^b R is defined as $[\sum(k^3\chi_{\text{exp}}(k) - k^3\chi_{\text{theor}}(k))^2 / \sum(k^3\chi_{\text{exp}}(k))^2]^{1/2}$.

**Figure 4.** Local structural parameters of the $\text{Cu}_2(\text{OH})_3^+$ layer.

C_2H_5),¹⁷ but the concluded changes in the interatomic distances are less than ~ 0.05 Å.

Magnetostructural Correlation. The magnetostructural correlation in the double hydroxo-bridge $\text{Cu}(\text{II})$ dinuclei complexes has been studied extensively. There is a linear relation between the magnetic exchange coupling constant J and the Cu–O–Cu bridge angle Δ : the ferromagnetic interaction of $J = 172 \text{ cm}^{-1}$ at $\Delta = 95.5^\circ$ is weakened by increasing the angle by $74 \text{ cm}^{-1}/\text{deg}$ and becomes to antiferromagnetic above $\Delta = 97.5^\circ$.¹⁸ The materials studied in this work involve similar local structures: the neighboring Cu^{II} ions are connected by two OH bridges whose Cu–O–Cu angle is expressed by the angle Δ in Figure 4. The angle Δ in these materials can uniquely be determined from the obtained distances in Tables 1 and 2 to be $\Delta = \sim 100^\circ$ for the $m = 0$ and 1 materials and $\Delta = \sim 92^\circ$ for the $m = 7\text{--}9$ materials. By applying the relation between Δ and J , the magnetic coupling between the Cu^{II} ions would be calculated to be -130 cm^{-1} for the shorter chain materials and $+462 \text{ cm}^{-1}$ for the longer chain materials, although such a straightforward application from the dinuclei system to the polymeric system has not been confirmed to make sense. As mentioned in the Introduction, the principal magnetic interaction

changes from ferromagnetic to antiferromagnetic with the extension of the alkyl chain. The calculated change of the $\text{Cu}^{\text{II}}\text{–Cu}^{\text{II}}$ magnetic interaction is completely opposite to the observation. Since there is no clue to estimate the interactions between $\text{Cu}^{\text{I}}\text{–Cu}^{\text{I}}$ and $\text{Cu}^{\text{I}}\text{–Cu}^{\text{II}}$ at this stage, it is hard to evaluate the application and, of course, to make a one-to-one relation between magnetism and structure. However, it is easily speculated that the concluded structural modification is large enough to explain the turnaround of the magnetic interaction, taking account of the empirical relation in the dinuclei system. In other words, the present EXAFS study strongly suggests that the observed magnetic change is not due to the change in the interlayer interaction but due to the intralayer structural modification.

Summary

We have measured the Cu K-edge EXAFS spectra of $\text{Cu}_2(\text{OH})_3\text{NO}_3$ and $\text{Cu}_2(\text{OH})_3(n\text{-C}_m\text{H}_{2m+1}\text{COO})$ ($m = 0, 1, 7, 8, 9$) at 20 K. Comparison of the observed spectra clearly indicates that the local structures in the $\text{Cu}_2(\text{OH})_3\text{NO}_3$ and the shorter chain materials ($m = 0, 1$) are quite similar to each other, while they are significantly different from those in the longer chain materials ($m = 7\text{--}9$). From the EXAFS analyses, the most significant change in the longer chain materials is concluded to be the contraction of the axial Cu–O bond. The change seems to result from the “chemical force” from the longer alkanecarboxylate to the bond, which also causes the cooperative structural modifications in the other parts. Such a large structural modification in the $\text{Cu}_2(\text{OH})_3^+$ layer may induce the drastic magnetic change found in the previous study.⁶ In the $\text{Cu}_2(\text{OH})_3(n\text{-C}_m\text{H}_{2m+1}\text{COO})$ system, the interlayer organic molecule would affect the intralayer structure and magnetic properties through the coordination. This is regarded as a new type of organic/inorganic cooperation and may open the possibility of controllable magnetic materials in future.

Acknowledgment. We thank Dr. S. Bando of Institute for Molecular Sciences for the TEM photography measurements and Prof. W. Mori of Kanagawa University for helpful discussion. This work has been performed under the approval of the Photon Factory Program Advisory Committee (PF-PAC 95-G192) and has been supported by a Grant-in-aid for Scientific Research from the Ministry of Education, Science, and Culture, Japanese government.

(17) Choy, J.-H.; Yoon, J.-B.; Kim, D.-K.; Hwang, S.-H. *Inorg. Chem.* **1995**, *34*, 6524.

(18) Kahn, O. *Molecular Magnetism*; VCH Publishers (UK) Ltd.: Cambridge, England, 1993; p 159.